Laser-Beam-Scattering Measurement of Ion Temperature in a θ-Pinch Plasma and Evidence for Thermonuclear Reactions

P. K. John*
Division of Pure Physics, National Research Council of Canada, Ottawa, Canada
(Received 18 October 1971)

Results are reported on an experiment to measure the ion temperature in a 100-kJ θ-pinch deuterium plasma. A ruby laser was used for scattering observations at 5° and 90° using multichannel spectrum analyzers and gave $n = 1.05 \times 10^{17}$ cm^{-3} and $T_i = 300$ eV. An independent measurement of the density was made by means of Rayleigh scattering. The neutron yield from the plasma was measured to be 8×10^8 sec^{-1}. The observed neutron emission was compared with that expected from a plasma with an ion temperature of 300 eV and was found to be of thermonuclear origin.

I. INTRODUCTION

It has always been recognized that light scattering would be an ideal technique for plasma diagnostics since it would make possible space-resolved measurements of plasma parameters without introducing any perturbations to the plasma itself. Since the cross section for Thomson scattering is extremely small, no suitable light source of sufficient intensity has been available until the development of the laser.[1] In giant pulse lasers one has an ideal source with the possibility[2] for the first time of measuring plasma parameters with true space and time resolution; space resolution of the order of millimeters and time resolution of the order of 10^{-8} sec.

The nature of the scattered spectrum depends on the value of the scattering parameter[3] α defined as

$$\alpha = \lambda_0 (ne^2/4\pi\kappa T_e)^{1/2} \, (1/\sin\tfrac{1}{2}\theta) \, ,$$

where λ_0 is the incident wavelength, n the electron density, T_e the electron temperature, and θ the angle of scattering. For a thermal plasma for $\alpha \ll 1$ the scattered spectrum has a Gaussian shape whose half-width is a measurement of the electron temperature. In addition to measuring the electron temperature, the electron velocity distribution may also be measured.[4] Since the scattered spectrum in the presence of a magnetic field is modulated[5] at the electron gyrofrequency, one can, by resolving this fine structure, measure the magnetic field[6] inside a plasma with true space resolution. For finite values of α, in the neighborhood of $\alpha \simeq 1$, the shape of the scattered spectrum is very sensitive to changes in the α value, and so in addition to the electron temperature, density can also be simultaneously determined from the same scattering spectrum by a best fit of the experimental data to the theoretical profiles. For $\alpha \gg 1$, the scattering is governed by collective effects, the spectrum now characteristic of electrons moving at the ion thermal speed, and the half-width of the scattered spectrum now dependent on the ion temperature T_i. The shape of the spectral profile measuring T_i under the condition $\alpha \gg 1$ is dependent on the ratio T_e/T_i, and hence T_i and T_e can both be measured simultaneously by a best-fit analysis of the experimental points to theoretical profiles. The satellite peaks appearing in the scattered spectrum for $\alpha \gg 1$ may be spectrally resolved to study damping[7] mechanisms in plasmas. Influence of density fluctuations on anamolous diffusion[8] may be studied by a knowledge of the Fourier sum of the squared density fluctuations, which is a quantity measured directly in a scattering experiment. In addition, since electron drift velocities introduce asymmetries in the scattered spectrum,[9,10] from the shape of the spectral profile, drift velocities may be measured too.

The first laboratory experiment on laser scattering was reported by Fiocco and Thomson[11] by scattering a ruby laser beam from an electron beam. Scattering from a laboratory plasma was reported by Funfer, Kronast, and Kunze[12] on a θ-pinch plasma at a scattering angle of 90°. Spectrally resolved scattering measurements were reported by Davies and Ramsden,[13] the scattered spectrum showing a Gaussian profile characteristic of plasma electrons in thermal equilibrium for $\alpha \ll 1$. Several other papers[14–17] have appeared reporting measurements of the electron temperature, density, and velocity distributions under the condition $\alpha < 1$ on a variety of plasmas. The last paper also discusses the problem of laser-induced plasma changes.

Experiments to observe cooperative effects in scattering have been performed mostly at small-angle forward scattering to satisfy the condition $\alpha \gg 1$ as was reported first by Ascolli-Bartolli, Katzenstein, and Lovisetto[18,19] and by DeSilva, Evans, and Forrest[20] obtaining evidence for the existence of the expected central-ion feature.

Chan and Nodwell,[21] doing a 45° scattering on a plasma jet, observed the two satellites, while Ramsden and Davies[22] working on a θ-pinch plasma were able to detect the ion feature and resolve the satellites. In both the latter experiments the widths of the satellites were considerably higher than the theoretical value, possibly due to nonuniform plasma density in the scattering region. Observations with $\alpha \sim 1$ were reported by Evans, Forrest, and Katzenstein[23] and by Anderson[24] obtaining both T_e and n by a least-squares fit to the theoretical profile. Forward-scattering measurements spectrally resolving the ion peak and thus measuring the ion temperature were first reported by Ramsden, Benesch, Davies, and John.[25] Further measurements were reported by Kronast, Rohr, Glock, Zwicker, and Funfer,[26] by John, Ramsden, and Benesch,[27] by Ramsden, John, Kronast, and Benesch,[28] by John and Kronast,[29] and by Daehler and Ribe[30] by using multichannel detection systems. All but one of these studies was also aimed at comparing the measured ion temperature[25,27-30] with the ion temperature calculated from the observed neutron emission, assuming a thermal plasma.

In this paper we describe the experimental determination of the ion temperature on a 100-kJ θ-pinch deuterium plasma by a forward-scattering measurement with the conditions $\alpha = 7.2$ in conjunction with an independent 90° scattering measurement of the electron temperature and density for $\alpha = 0.44$. The ion temperature thus measured is compared with that calculated from the neutron-emission rate from the plasma as measured by a calibrated neutron detector.

II. THEORY

Scattering of electromagnetic radiation by a medium[31,32] is due to density fluctuations, and the problem of scattering of light by plasmas has been considered in detail by several authors.[3,9,33-35] The quantity measured in a scattering experiment is the spatial Fourier transform of the charge density and the spectral distribution of the scattered radiation is given by[3,33]

$$\pi^{1/2} I(\omega')\, d\omega' = \Gamma_\alpha(x)\, dx + Z[\alpha^2/(1+\alpha^2)]^2\, \Gamma_\beta(y)\, dy\ , \tag{1}$$

where $x \equiv \omega'/\omega_e$ and $y \equiv \omega'/\omega_i$, with ω' the Doppler shift in frequency, $\omega_e = k(2\kappa T_e/m_e)^{1/2}$ and $\omega_i = k(2\kappa T_i/m_i)^{1/2}$, where κ is the Boltzmann constant, m_e and m_i are the electron and ion masses, and $k = 2k_0 \sin\frac{1}{2}\theta$, with k_0 the wave number of the incident radiation. The term $\Gamma_\alpha(x)$ in Eq. (1), is given by

$$\Gamma_\alpha(x) = \frac{e^{-x^2}}{[1+\alpha^2-\alpha^2 f(x)]^2 + \pi\alpha^4 x^2 e^{-2x^2}}\ , \tag{2}$$

in which

$$f(x) = 2xe^{-x^2}\int_0^x e^{t^2}\, dt$$

represents the spectrum of scattering by free electrons with spectral width ω_e or the so-called "electron component." The second term $\Gamma_\beta(y)$, given by a function of the same form as Γ_α when α is replaced by

$$\beta \equiv \left(\frac{Z(T_e/T_i)\alpha^2}{1+\alpha^2}\right)^{1/2}$$

and x is replaced by y, represents the spectrum of scattering by electrons moving in phase with the ion or the ion component of the spectrum having a spectral width ω_i. It is easily seen from the above equations that the shape of the electron component of the scattered spectrum is strongly dependent on the parameter α and the shape of the ion component on the parameter β. However, for a nonthermal plasma the shape would also be affected by an electron drift velocity.[10] The total scattered intensity is

$$I = \int I(\omega')\, d\omega' \equiv I_e + I_i\ , \tag{3a}$$

where I_e and I_i are the intensities of the electron and ion components and are given by

$$I_e = 1/(1+\alpha^2) \tag{3b}$$

and

$$I_i = \frac{Z\alpha^4}{(1+\alpha^2)[1+\alpha^2+Z(T_e/T_i)\alpha^2]}\ . \tag{3c}$$

It follows immediately from the above three equations that for $\alpha \ll 1$, the intensity $I \simeq I_e$, the scattered intensity being almost exclusively in the electron component with $I_i \simeq 0$, and for $\alpha \gg 1$, $I \simeq I_i$, with $I_e \simeq 1/\alpha^2$, most of the contribution to the scattering coming from the ion component.

III. CHOICE OF PARAMETERS

Since α is proportional to $1/\sin\frac{1}{2}\theta$, for a given plasma one changes from a small α value to a large α value by changing from a large scattering angle to a small angle or forward scattering. Experimentally the most convenient large-angle scattering is 90° and for many laboratory plasmas of interest including the θ-pinch plasma under investigation here, $\theta = 90°$ satisfies the condition $\alpha < 1$. Figure 1 shows a family of graphs of α as a function of n for a wide range of temperatures and different scattering angles θ. It is also clear from the figure that for plasmas of density and temperature of orders of magnitude $10^{17}/\text{cm}^3$ and 10^6 °K the condition $\alpha > 1$ is achieved for $\theta < 10°$. Since the width of the scattered spectrum is proportional to $\sin\frac{1}{2}\theta$ and $T^{1/2}$, it is easily seen that the half-width of the ion component is proportional to α^{-1}, and Fig. 2 shows a set of graphs of the half-width $\Delta\lambda$

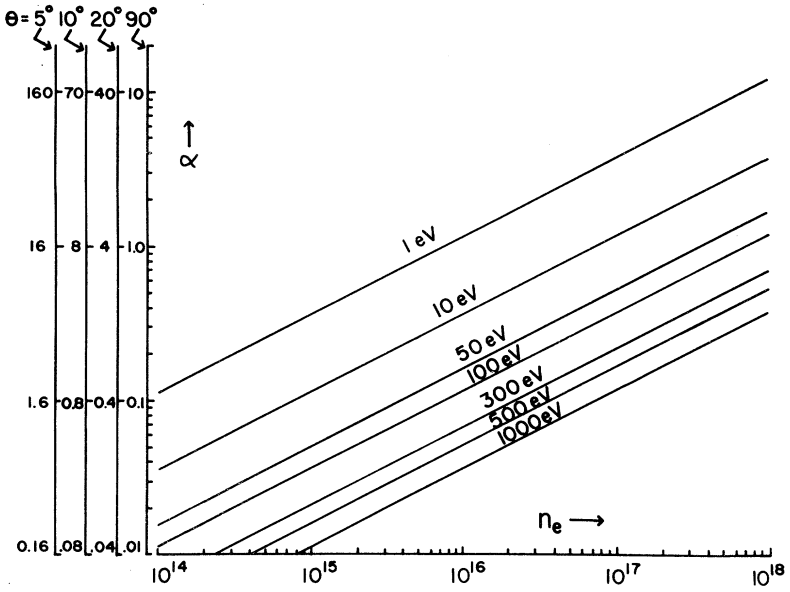

FIG. 1. Scattering parameter α as a function of electron density n for various values of T_e.

as a function of T_i for a range of scattering angles. Note that for a given ion temperature, the smaller the scattering angle θ, the smaller the width of the scattered spectrum, which puts a lower limit on the scattering angle θ to which one can go to increase α and an upper limit on the linewidth of the laser to be used in the scattering observations. The solid angle of viewing $\Delta\Omega$ also depends on the choice of α, and it is easily seen to be proportional to $(\Delta\alpha)\alpha^{-3}$, where $\Delta\alpha$ is the spread in α due to the finite angular spread $\Delta\theta$ necessary to provide the solid angle $\Delta\Omega$. In the present case for the forward scattering the angle was chosen to be 5°. The stray-light problem also becomes very severe as one goes to smaller angles.

IV. APPARATUS

A. General Setup

The laser used was a ruby laser with an effective power of 30 MW and pulse width of 50 nsec. The linewidth and wavelength stability were better than 0.1 Å. A general schematic of the experimental setup is shown in Fig. 3. The simulated laser beam shown in the diagram was used in the optical alignment of the system. The lenses used were all selected better-quality Bausch and Lomb plano-convex lenses. A and A_1 were brass apertures and B_1 and B_2 ordinary microscope slide beam splitters. The aperture A limited the beam divergence of the laser to 3 mrad. The laser wavelength monitor was a Fabry-Perot interferometer measuring the linewidth and wavelength stability by photographing the ring pattern. Aperture A_1 further ensured that the beam divergence was limited to 3 mrad. Lens L_4 finally refocused the beam at the midplane of the θ-pinch coil to a diameter of 6 mm. The direct laser beam was finally absorbed in the laser dump which was a Chance-Pilkington OB10 blue filter glass at Brewster angle at the end of a 30-cm-long glass tube.

B. Detection System

1. Forward Scattering

Light scattered at 5° to the forward direction was collected by a quartz axicon[36] which is basically a thin prism of revolution and has the property of collimating light from a finite length along the

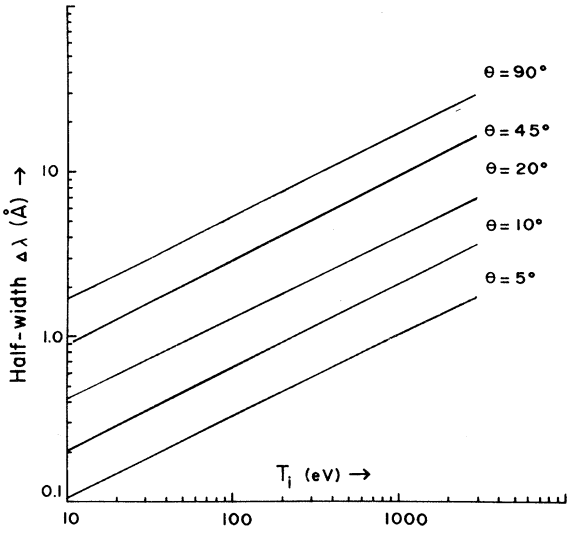

FIG. 2. Half-width $\Delta\lambda$ of the scattered spectrum (assuming Gaussian) as a function of the ion temperature T_i for different values of θ.

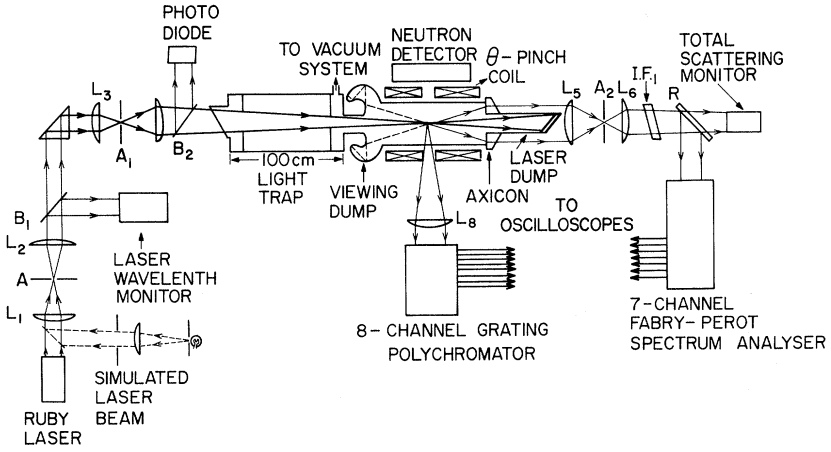

FIG. 3. General schematic of the scattering experiment.

axis. The scattered rays rendered parallel to the axis by the axicon was then focused by lens L_5 at A_2. The length of the plasma column observed which is limited essentially by an annular masking aperture on the axicon was ~ 12 cm. The viewing dump was made up of two concentric glass flasks and painted black to provide a black background for the detection optics. Light from A_2 rendered parallel by lens L_6 was passed through a 4-Å half-width interference filter IF_1 centered at the laser wavelength which was used to block off the plasma continuum outside its pass band. A photomultiplier placed behind the partially transmitting reflector R collected ~ 15% of the total scattered light which gave a measure of the total light scattered by the plasma. The light reflected by R was dispersed by a pressure-tuned Fabry-Perot interferometer and measured by a seven-channel detection system.[37] The system was similar in principle to the one described by Hirschberg and Platz[38] and used by Daehler, Sawyer, and Thomas[39] and recorded the complete spectrum of the scattered laser light in a single shot. The resolution of the system was 0.2 Å.

2. 90° Scattering

An eight-channel polychromator similar to the one described by Glock *et al.*[40] was used and the setup was as shown in Fig. 4. Scattered light at 90° was collected over a length of 7 mm by the lens L_8 through a slot in the θ-pinch coil and after reflection by a 10-Å half-width interference filter IF_2 which was set for peak transmission at the laser wavelength was focused onto one end of a fiber optic bundle of diameter of 3 mm. The other end of the fiber optic was a slit 1 cm × 0.75 mm and formed the entrance slit of the polychromator. The exit slits were also fiber optics of the same dimensions and had a spectral width of 55 Å per channel.

3. Neutron Detector

The neutron detector used was a polished NE-102 plastic scintillator 3 × 6 × 12 in. in conjunction with a photomultiplier. The scintillator-photomultiplier assembly was properly shielded against x rays and magnetic fields. The detector was calibrated in position by using an Am-Be source with a total neutron flux of 10^6/sec. Calibration was established for the count rate of scintillator pulses and also for the mean current drawn by the detector when irradiated by the Am-Be source and these calibrations agreed to within 20%. An independent check was made using a BF_3 Counter.

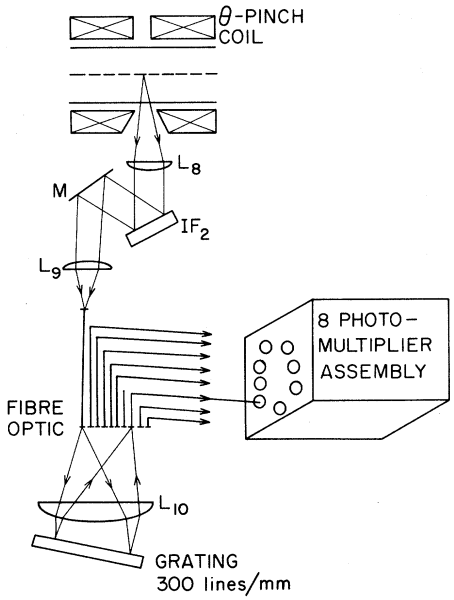

FIG. 4. Details of the eight-channel grating polychromator used in the 90° scattering measurement.

C. Problem of "Stray Light"

One of the problems in a laser-scattering experiment arises from the extremely small cross section for Thomson scattering, a consequence of which is that from typical plasmas approximately only 10^{-12} to 10^{-10} of the incident radiation is scattered. Great care therefore has to be taken to prevent any direct laser light or "stray light" from getting into the detector. We list below some of the precautions that were taken by which the stray-light level was reduced to less than 10% of the scattered signal in the forward-scattering case. The lenses were tilted ~5° and were also apertured just sufficiently to let the laser beam through. The use of two "clean-up" apertures A and A_1 was a most important factor in reducing stray light. The alignment of A_1 was very critical and any slight misalignment was manifested as almost an order of magnitude increase in the stray-light level. There were two apertures in the light trap and the Brewster-angle entrance window was not in the line of sight of the axicon. A properly aligned viewing dump was a very important factor in reducing the stray light. The whole optical path was divided into several optically isolated regions by black partitions. Use of interference filter IF_2 (Fig. 4) as a reflector helped to reduce stray light in the 90° scattering by an order of magnitude.

D. Systems Check and Calibration

The magnitude of the stray-light level was determined by comparing it with Rayleigh scattering from nitrogen. Rayleigh-scattered light was used also in the gain calibration of the channels of the forward-scattering system. Wavelength calibration and measurement of resolution and spectral width of the system were also made using the laser light by pressure scanning of the Fabry-Perot with nitrogen. Gain adjustments of the photomultipliers of the polychromator were made using the plasma continuum radiation as the light source with appropriate corrections added to the different rise-time responses of the electronics of each channel, and the laser light being used for wavelength calibration.

E. θ-Pinch

The plasma was produced in a 100-kJ θ pinch with deuterium at 60-mTorr pressure in a discharge tube with an internal diameter of 5.8 cm. The coil length was 38 cm with an internal diameter of 6.5 cm. A reverse B_z field of 3.5 kG and quarter period 24 μsec was first applied and 1.5 μsec later the gas was preheated by discharging a 0.5-μF capacitor at 17.7 kV. This was followed 20 μsec later by discharging the main capacitor banks of 510 μF at 19 kV. The preheater and main banks had quarter periods of 0.22 and 6 μsec, respectively, and the peak magnetic field was 72 kG, corresponding to a peak current of 2.4×10^6 A. The gas pressure and reverse B_z were chosen to give the maximum neutron yield.

V. EXPERIMENTAL PROCEDURE

The Fabry-Perot is pressure tuned to transmit the laser light and have it centered on any given channel, in our case the fourth channel, as observed by the stray-light signal. Then the plasma is fired and at the desired time in the discharge the laser is fired. In a single firing the following observations are made and are shown in Fig. 5. in the forward-scattering case: the signals on the Fabry-Perot seven channels, the total scattering monitor, the interferogram on the laser wavelength monitor, the laser amplitude by diode monitor, and the signal from the neutron-detector scintillator. In a separate shot for 90° scattering, corresponding data for the eight channels of the polychromator were obtained. Stray-light measurements were taken before and after each scattering observation, as a continuous check on the stray-light level and wavelength calibration. The true scattering signal for each channel is obtained by subtracting the stray-light signal for the corresponding channel. A number of shots were taken at different times in the discharge. For an independent measure of plasma-density, Rayleigh-scattering measurements were taken at a pressure of 300 mTorr of nitrogen. The experimental-scattering profiles obtained are compared with theoretical profiles after being folded onto the instrumental profile and temperature and density obtained by a best-fit analysis.

VI. RESULTS AND DISCUSSIONS

A. Temperature and Density

In principle one can determine the ratio of the electron temperature to the ion temperature from the shape of the forward-scattered spectrum and the ion temperature T_i from its absolute width, provided the electrons and the ions are in separate thermal equilibrium. But in our case of a low T_e/T_i value (which was about 0.45) the shape of the spectrum, while not affected by a drift velocity of up to half the thermal velocity, was very insensitive to changes in the ratio T_e/T_i, and the corresponding error brackets did not allow for an accurate determination of the ion temperature T_i. Therefore an independent determination of T_e was essential and was made by performing the 90° scattering measurement. The spectra of light scattered at 5° and 90° to the forward direction are shown in Fig. 6 and were taken between 4 and 5 μsec after the beginning of the plasma discharge,

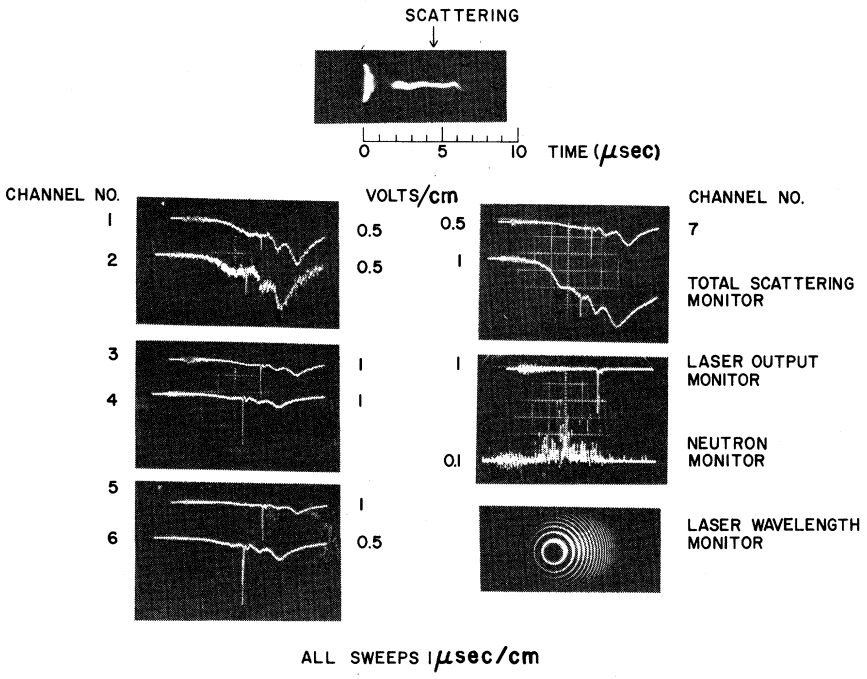

FIG. 5. Typical data recorded simultaneously in a single-plasma discharge showing the scattering signals on the seven photomultipliers of the Fabry-Perot multichannel system, the signal on the photomultiplier monitoring the total scattered signal, the photodiode signal monitoring the laser output, the signal on the neutron-detector, Fabry-Perot interferogram monitoring the wavelength stability and linewidth of the laser, and also the time-resolved streak photograph of the plasma taken at the midplane of the θ-pinch coil.

corresponding to the time of peak neutron emission. The points are averaged over a number of shots and thus the standard deviations indicate both the error in the measurements and the irreproducibility of the plasma. The 90° spectrum refers to a 7-mm-long plasma region in the center of the coil, and the scattered light was taken over the whole cross section of the plasma which was reasonably homogeneously illuminated by the laser beam. A best-fit analysis of the spectrum was made after taking into account the instrumental width of the polychromator and gave an electron temperature at 4.5 μsec, which corresponded to the time of peak neutron emission, of $T_e = 75^{+23}_{-16}$ eV and $\alpha = 0.44^{+0.1}_{-0.15}$, with the electron density $n = (1.3 \pm 0.35) \times 10^{17}$ cm^{-3}. The above measured electron temperature for use in conjunction with the forward-scattering data, had to be corrected for the fact that in the case of the forward scattering the temperature is averaged over a 12-cm length of the plasma column. Time-resolved measurements of the electron temperature between 3 and 5 μsec showed that T_e at the center of the coil had at least a tendency to fall off slightly with time even before the peak magnetic field was attained at 6 μsec, indicating that while there was still a trapped antiparallel magnetic field at 4.5 μsec there was already some particle loss at this time. Hence the correction for the measured electron temperature to get a mean for the 12-cm length was made by interpolating between the case of negligible end losses and the lossy case of no antiparallel trapped field as was reported by Beach[41] for a similar θ pinch. This gave the space-averaged value for the 12 cm length of the plasma column to be 67^{+21}_{-15} eV. Also, in the 90° scattering case, experimental conditions were such that the preheater and main bank capacitor voltages were higher by about 10 and 5%, respectively, with respect to the forward-scattering case. Therefore a correction[42] had to be applied to the above value of T_e and accordingly the corrected value appropriate to the forward-scattering conditions was obtained to be $T_e = 60^{+18}_{-13}$ eV.

In Fig. 6(a), the forward-scattering spectrum is shown. A best-fit analysis of the spectrum including a convolution of the measured Lorentzian instrumental profile was made for different values of the ion temperature T_i corresponding to various values of the ratio T_e/T_i. With the already determined value of $T_e = 60$ eV, this gave the value of the ion temperature as $T_i = 300 \pm 50$ eV.

The average value of the electron density n over the 12 cm length of the forward-scattering region was calculated making the reasonable assumption that n/T is a constant to a good approximation and hence α is a constant over the 12-cm length. From the average T_e value the corresponding n value was calculated and gave

$$n = 1.05 \times 10^{17} \text{ cm}^{-3} .$$

An independent measurement of the electron density, or rather, the total number of electrons in the forward-scattering volume was made from a comparison of the total scattering in the forward direction with Rayleigh scattering from dust-free nitrogen at a pressure of 300 Torr. The cross

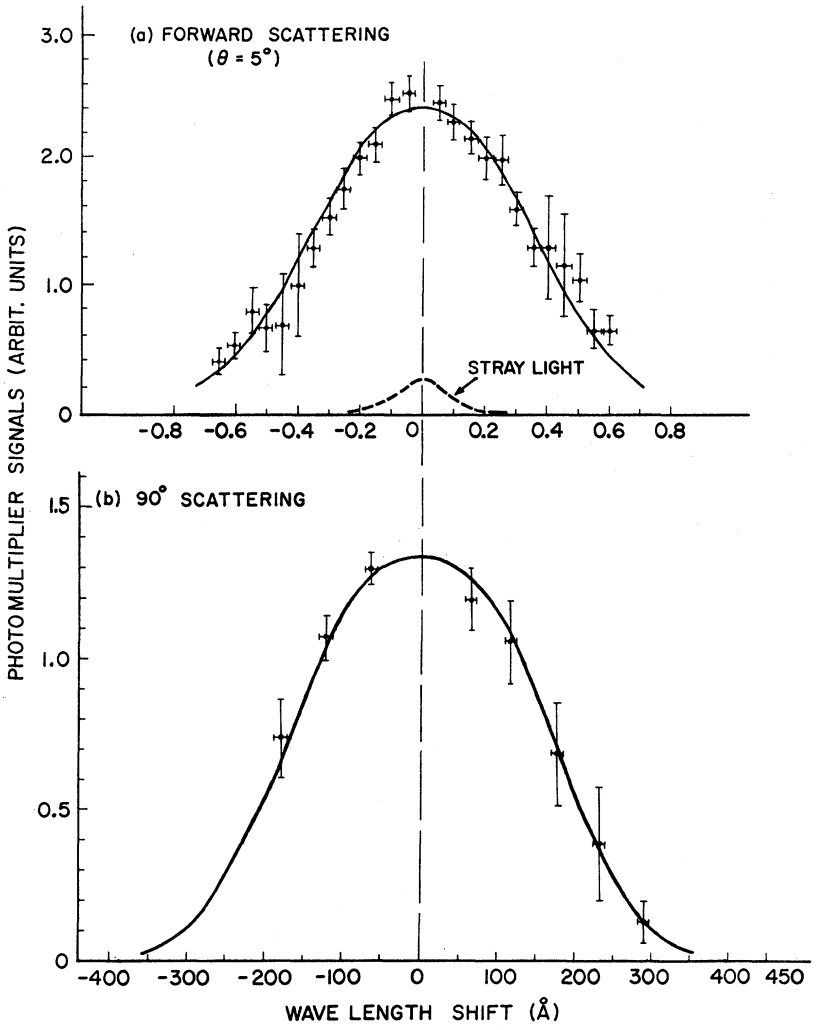

FIG. 6. Scattering results. The solid curve is the best fit of the experimental points to the theoretical profiles: (a) forward scattering at $\theta = 5°$ for $T_i = 300$ eV and $T_e = 60$ eV; (b) 90° scattering for $T_e = 75$ eV and $\alpha = 0.44$.

section σ_R for Rayleigh scattering[43] is given by

$$\sigma_R = (32\pi^3/3n_R)(\mu - 1)^2/\lambda_0^4 ,$$

where μ is the refractive index of the gas at a particle density n_R and λ_0 is the incident wavelength. The effective Thomas-scattering cross section in the forward direction is given by $\sigma_{\text{eff}} = \sigma_e I_i$, where σ_e is the single-electron Thomson-scattering cross section and I_i is defined in Eq. (3c) earlier. The frequency-integrated total-scattering signal I_S from a scattering region containing a total of N_e electrons is given by

$$I_S = (I_i \sigma_e) N_e ,$$

and the total Rayleigh-scattered signal I_R from the same scattering region containing N_R molecules is $I_R = \sigma_R N_R$, so that

$$N_e = (1/I_i)(I_S/I_R)(\sigma_R/\sigma_e) N_R = nV ,$$

where V is the volume of the scattering region. The ratio of Rayleigh-scattering cross section to the Thomson-scattering cross section σ_R/σ_e equals 1/377. In our case $I_i = 0.8$ and with the experimentally measured value of the ratio of the total Thomson-scattered signal to the Rayleigh-scattered signal in the forward direction $I_S/I_R = 0.86$, one gets from the above equation $nV = 8.3 \times 10^{16} \pm 50\%$. The error of 50% is due to the error in the measurements of I_S/I_R and the error in the absolute calibration of the gauge reading the nitrogen pressure. It might be worth mentioning that the θ-pinch plasma turned out to be hollow as is to be expected from the antiparallel field of 3.5 kG, part of which was still trapped inside the plasma at the scattering time of 4.5 μsec.

B. Neutron Yield

1. Observed Neutron Emission

The neutron emission from the plasma was measured by the calibrated NE102 plastic scintillator. Over the several shots considered the neutron emission fluctuated appreciably, sometimes

giving a measureable current and at other times the output signal consisted of individual pulses. The average neutron yield as measured was $(8 \pm 6) \times 10^8$ sec^{-1}.

2. Expected Neutron Yield

For a plasma in thermal equilibrium, the total number of neutrons N emitted is given by

$$N = \int dV (\tfrac{1}{2} n_i^2 \langle \sigma v \rangle_{DD}) = \tfrac{1}{2} n_i (n_i V) \langle \sigma v \rangle_{DD} ,$$

where n_i is the density of deutrons, $n_i V$ is the total number of reacting particles, and $\langle \sigma v \rangle_{DD}$ is the average value of the D-D reaction cross section[44] corresponding to the plasma-ion temperature. From Rayleigh scattering, $nV = 0.81 \times 10^{17}$ over a 12 cm length of plasma column. With the coil length of 38 cm it was considered reasonable to assume a neutron-emitting length of 30 cm; the temperature drop beyond which would make its contribution of neutrons lower by more than an order of magnitude, and extrapolating from the total number of ions, nV, in the scattering region of length 12 cm, one obtains the total number of interacting ions to be $n_i V = 2.8 \times 10^{17}$, and the total number of neutrons expected at an ion temperature of 300 eV turns out to be 4×10^8/sec. Taking into account the ± 50-eV standard deviation in the ion temperature of 300 eV would give the expected neutron emission as between 1×10^8 to 2×10^9 per second. This has now to be compared with the observed average neutron-emission rate of $(8 \pm 6) \times 10^8$/sec. Within the limits of the error then, the observed neutron-emission rate is in agreement with that expected from a thermonuclear plasma at the measured temperature of 300 eV, thus giving the closest agreement yet between directly measured neutron yield and that calculated from plasma parameters measured by scattering from a laboratory plasma. This is additional evidence for the thermonuclear origin of the neutron emission from a θ-pinch plasma.

ACKNOWLEDGMENTS

The author is indebted to Dr. S. A. Ramsden who initiated this work, for his continuous interest, and constant encouragement. Thanks are also due to Dr. B. Kronast for help towards the later stages of this work especially in the interpretation of the results, to R. Benesch for aid in performing the experiment, to W. J. Orr for help with the instrumentation, and to D. Coleman for computing assistance.

---

*Present address: Department of Physics, University of Western Ontario, London, Canada.

[1]T. H. Maiman, Nature 187, 493 (1960).
[2]T. P. Hughes, Nature 194, 268 (1962).
[3]E. E. Salpeter, Phys. Rev. 120, 1528 (1960).
[4]T. S. Brown and D. J. Rose, J. Appl. Phys. 37, 2709 (1966).
[5]T. S. Laspere, J. Geophys. Res. 65, 3955 (1960).
[6]D. E. Evans and P. G. Carolan, Phys. Rev. Letters 25, 1605 (1970).
[7]T. J. M. Boyd, United Kingdom Atomic Energy Authority Research Group Report No. CLM-R52 (unpublished).
[8]S. Yoshikawa and D. J. Rose, Phys. Fluids 5, 334 (1962).
[9]M. N. Rosenbluth and N. Rostoker, Phys. Fluids 5, 776 (1962).
[10]O. Theimer, Institüt fur Plasma Physik, Garching, Report No. IPP1/48:55, 1966 (unpublished).
[11]G. Fiocco and E. Thompson, Phys. Rev. Letters. 10, 89 (1963).
[12]E. Funfer, B. Krunast, and H. J. Kunze, Phys. Letters 5, 125 (1963).
[13]W. E. R. Davies and S. A. Ramsden, Phys. Letters 8, 179 (1964).
[14]H. J. Kunze, E. Eberhagen, and F. Funfer, Phys. Letters 13, 38 (1964).
[15]E. E. Schwarz, J. Appl. Phys. 36, 1836 (1965).
[16]R. M. Patrick, Phys. Fluids 8, 1985 (1965).
[17]E. T. Gerry and D. J. Rose, J. Appl. Phys. 37, 2715 (1966).
[18]U. Ascolli-Bartolli, J. Katzenstein, and L. Lovisetto, Nature 204, 672 (1964).
[19]U. Ascolli-Bartolli, J. Katzenstein, and L. Lovisetto, Nature 207, 63 (1965).
[20]A. W. DeSilva, D. E. Evans, and M. J. Forrest, Nature 203, 1321 (1964).
[21]P. W. Chan and R. A. Nodwell, Phys. Rev. Letters. 16, 122 (1966).
[22]S. A. Ramsden and W. E. R. Davies, Phys. Rev. Letters 16, 303 (1966).
[23]D. E. Evans, M. J. Forrest, and J. Katzenstein, Nature 211, 23 (1966).
[24]O. A. Anderson, Phys. Rev. Letters 16, 978 (1966).
[25]S. A. Ramsden, R. Benesch, W. E. R. Davies, and P. K. John, IEEE J. Quantum Electron. QE-2, 267 (1966).
[26]B. Kronast, H. Rohr, E. Glock, H. Zwicker, and E. Funfer, Phys. Rev. Letters 16, 1082 (1966).
[27]P. K. John, S. A. Ramsden, and R. Benesch, Bull. Am. Phys. Soc. 12, 743 (1967).
[28]S. A. Ramsden, P. K. John, B. Kronast, and R. Benesch, Phys. Rev. Letters 19, 688 (1967).
[29]P. K. John and B. Kronast, Bull. Am. Phys. Soc. 13, 1550 (1968).
[30]M. Daehler and F. L. Ribe, Phys. Rev. 161, 117 (1967).
[31]R. Bhagavantam, *Scattering of Light and the Raman Effect* (Chemical Publishing, New York, 1942).
[32]L. Rosenfeld, *Theory of Electrons* (Interscience, New York, 1951).
[33]E. E. Salpeter, J. Geophys. Res. 68, 1321 (1963).
[34]J. A. Fejer, Can. J. Phys. 39, 716 (1961).
[35]J. P. Dougherty and D. T. Farley, J. Geophys. Res. 68, 473 (1963).
[36]T. H. McLeod, J. Opt. Soc. Am. 44, 592 (1954).
[37]P. K. John and R. Benesch, Appl. Opt. 11, 153

(1972).
[38]J. G. Hirschberg and P. Platz, Appl. Opt. 4, 1375 (1965).
[39]M. Daehler, G. A. Sawyer, and K. S. Thomas, Phys. Fluids 12, 225 (1969).
[40]E. Glock, *Proceedings of the Seventh International Conference on Ionization Phenomena in Gases, Belgrade*, 1965 (Gradjevinska Knjiga Publishing House, Belgrade, Yugoslavia, 1965), Vol. 3, p. 194.
[41]A. D. Beach. J. Sci. Instr. 44, 690 (1967).
[42]C. Longmire, J. L. Tuck, and W. B. Thompson, *Plasma Physics and Themonuclear Research* (MacMillan, New York, 1965), Vol. 1, pp. 216–222.
[43]Lord Rayleigh, Phil. Mag. 47, 379 (1899).
[44]S. Glasstone and R. H. Loveberg, *Controlled Thermonuclear Reactions* (Van Nostrand, New York, 1960), p. 20.

PHYSICAL REVIEW A VOLUME 6, NUMBER 2 AUGUST 1972

Experimental Indications of Plasma Instabilities Induced by Laser Heating*

J. W. Shearer, S. W. Mead, J. Petruzzi, F. Rainer, J. E. Swain, and C. E. Violet
Lawrence Livermore Laboratory, University of California, Livermore, California 94550
(Received 20 December 1971)

The detection of ~ 100-keV x radiation and of directly back-scattered light is described for neodymium-glass-laser light pulses focused on a polyethylene target. These observations can be explained in terms of the nonlinear excitation of plasma waves by the laser light.

We recently made some measurements of x rays and light reflection from a laser-produced plasma which suggest that plasma instabilities have been produced. Our neodymium laser, which includes a multipass glass-disk system, has been described elsewhere.[1–3] The 1.06-μm-wavelength neodymium-laser light was focused by means of an $f/7$ lens to an irregular-shaped spot with a mean diameter of approximately 80 μm.[3] The pulse energy ranged from 20 to 70 J; the pulse length ranged from 2 to 5 nsec. The maximum power during the pulse was 10 GW, corresponding to an intensity at the target of $\simeq 2\times 10^{14}$ W/cm^2.

The laser pulse was focused on flat targets of "deuterated" and ordinary polyethylene, $(CD_2)_n$ and $(CH_2)_n$, respectively. The targets were tilted about 5° to prevent back reflections from causing spontaneous oscillations in the laser amplifier chain. After each shot the target was moved to expose a fresh new surface. It was found necessary to wait 1 h between shots to allow the disk laser to cool. Failure to allow ample cooling resulted in a larger focal spot and a decrease or an absence of neutrons and hard x rays.

Diagnostics for the first set of experiments included a large plastic scintillation counter, intended for neutron detection and located in close proximity to the laser target. The detector was initially shielded with 9.5 mm of aluminum plus 6.3 mm of lead. Nevertheless, when the laser was fired, scintillation pulses were seen from the $(CH_2)_n$ target as well as from $(CD_2)_n$. When the shielding thickness was increased to 9.5 mm of aluminum plus 12.7 mm of lead, no pulses were seen when the $(CH_2)_n$ target was in place, but small pulses corresponding to 10^3 and 10^4 neutrons were seen when the $(CD_2)_n$ target was used.[3–5]

The fact that large pulses were seen from a $(CH_2)_n$ target with a scintillation detector shielded by 6.3 mm of lead was interpreted as evidence that considerable quantities of hard x rays were being produced in these experiments. Similar hard x radiation has been reported recently by the Lebedev group in the USSR.[6]

To measure the x-ray spectrum more accurately, additional measurements were taken with four scintillation detectors using a target of polyvinyl chloride. One pair of detectors used europium-activated calcium fluoride fluors in conjunction with aluminum absorbers; the other pair used thallium-activated sodium iodide fluors and nickel absorbers. To minimize background corrections, the nickel-absorber pair was shielded from scattered hard x rays by at least 6 mm of lead on all sides, except for a narrow cone pointed at the focal spot. The aluminum-absorber pair did not need such shielding, because the soft-x-ray signal was much greater than the hard-x-ray background. The absorption ratios for a given absorber pair were normalized by means of supplementary measurements made with equal absorber thicknesses. An apparent electron temperature T was computed from the measured absorption ratio using the curves computed by Elton.[7]

Some representative results of these measurements are presented in Table I; they indicate that the transmission ratio for the nickel pair corresponds to a much higher temperature than the corresponding ratio for the aluminum pair. In addition to the results given in the table, we made a

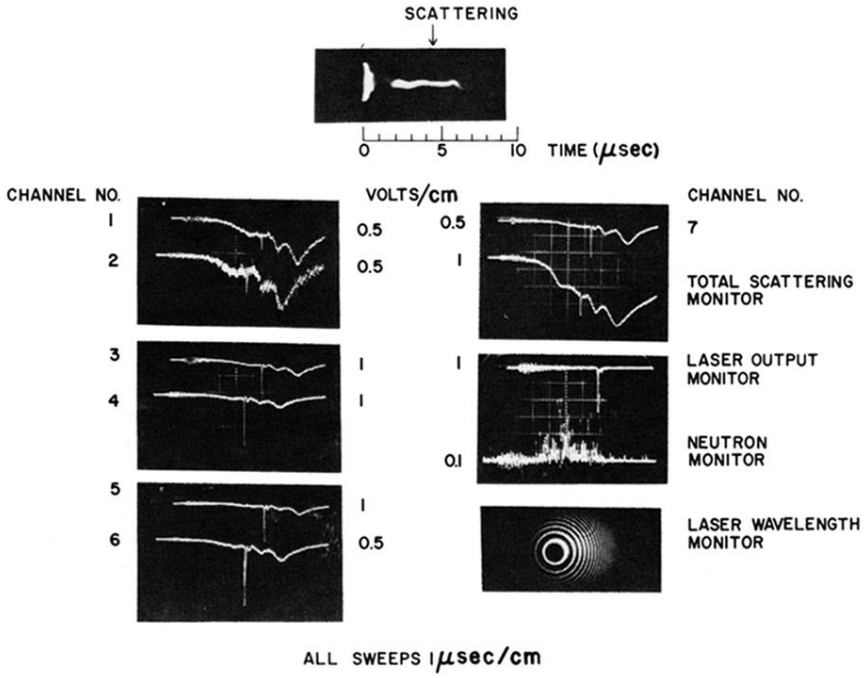

FIG. 5. Typical data recorded simultaneously in a single-plasma discharge showing the scattering signals on the seven photomultipliers of the Fabry-Perot multichannel system, the signal on the photomultiplier monitoring the total scattered signal, the photodiode signal monitoring the laser output, the signal on the neutron-detector, Fabry-Perot interferogram monitoring the wavelength stability and linewidth of the laser, and also the time-resolved streak photograph of the plasma taken at the midplane of the θ-pinch coil.